Available online at www.sciencedirect.com
ScienceDirect
Journal of Hazardous Materials 146 (2007) 204–213
Journal of Hazardous Materials
www.elsevier.com/locate/jhazmat

Photocatalytic degradation of triazophos in aqueous titanium dioxide suspension: Identification of intermediates and degradation pathways

T. Aungpradit [a], P. Sutthivaiyakit [a,*], D. Martens [b,c], S. Sutthivaiyakit [d], A.A.F. Kettrup [b,c]

[a] *Postgraduate Education and Research Program in Analytical Chemistry, Department of Chemistry, PO Box 1011 Kasetsart, Kasetsart University, Bangkok 10903, Thailand*
[b] *Department of Ecological Chemistry and Environmental Analysis, Technical University of Munich, D-85350 Freising-Weihenstephan, Germany*
[c] *Institute of Ecological Chemistry, GSF-National Research Centre for Environment and Health, Ingoldstaedter Landstrasse 1, 85764 Neuherberg, Germany*
[d] *Department of Chemistry, Faculty of Science, Ramkhamhaeng University, Bangkok 10240, Thailand*

Received 17 October 2006; received in revised form 1 December 2006; accepted 4 December 2006
Available online 8 December 2006

Abstract

The photocatalytic degradation of triazophos in aqueous TiO_2 suspension has been studied in a photoreactor operating with simulated solar radiation. The decrease in triazophos concentration followed first-order kinetics with a half-life of 4.76 ± 0.42 h at a TiO_2 suspension concentration of 10 mg/L. Seventeen degradation products were identified using HPLC-UV, HPLC/MS/MS, GC/MS/MS and IC, and by comparing retention times and spectra with commercially available authentic standards. On the basis of the observed transformation products, two routes were proposed, one based on the initial oxidative cleavage of P=S bond to P=O bond, and the other on initial cleavage of the ester P–O bonds. Photocatalysis holds promise for the solar treatment of pesticide-contaminated waters.

Keywords: Photocatalytic degradation; Triazophos; HPLC/MS/MS; TiO_2; Simulated solar irradiation

1. Introduction

Triazophos is the common name for *O*,*O*-diethyl-*O*-1-phenyl-1H-1,2,4-triazol-3-yl phosphorothioate (Fig. 1). It is used on various crops such as cotton and rice to control aphids, fruit borers, leave hoppers and cut worms. It is a moderately toxic and broad spectrum, nonsystemic organophosphorus pesticide [1–2] and is used in large quantities throughout the world.

Previous research has shown that triazophos undergoes degradation through a variety of conditions [3–5]. Triazophos in canal water (pH 8.3) degraded with a half-life of approximately 25.44 days [3]. Triazophos degraded more rapidly in a photo-Fenton system to a series of degradation products and five major products, for example, *O*,*O*-diethyl phosphorothioic acid, monoethyl phophorothioic acid, phosphorothioic acid, 1-phenyl-3-hydroxy-1,2,4-triazole and phenyl semicarbazide were identified as their corresponding trimethylsilyl derivatives with gas chromatography–mass spectrometry [4]. Two different hydrolysis pathways in acid and neutral solutions, and in basic solution were proposed [5].

Although photolysis and hydrolysis eventually result in loss of triazophos, the reactions are relatively slow and are unlikely to be useful in the treatment of pesticide-contaminated water. Degradation of triazophos by sunlight in the presence of titanium dioxide may provide a cost-effective treatment method for triazophos-contaminated water. Photocatalysis with TiO_2 has been studied for over 20 years and has been used for a number of water treatment applications [6]. The technology is attractive as solar energy is an inexpensive, renewable energy source and is particularly relevant for agricultural countries like Thailand where it may be necessary to treat water in the absence of a reliable electricity source. Furthermore, it can lead to complete mineralization [7–9], thereby eliminating potential effects associated with toxic intermediates. Although there have been reports on degradation of pesticides [8–13] in polluted waters, the efficiency of the process is heavily dependent on the chemical nature of the pesticides being treated. The present work aims to study the kinetics, to identify intermediates and to propose degradation mechanism of photocatalytic degradation of triazophos using simulated solar radiation.

* Corresponding author. Tel.: +662 9428900x632/607; fax: +662 5790658.
E-mail address: fscipws@ku.ac.th (P. Sutthivaiyakit).

0304-3894/$ – see front matter © 2006 Elsevier B.V. All rights reserved.
doi:10.1016/j.jhazmat.2006.12.007

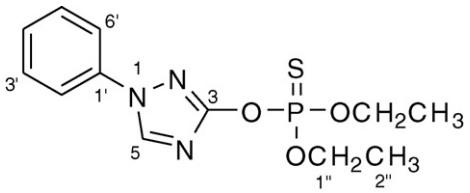

Fig. 1. Structure of triazophos.

2. Experimental

2.1. Materials

Triazophos (97%), 1-phenyl semicarbazide (99%) and acetonitrile (HPLC grade) were obtained from Dr. Ehrensdorfer, Aldrich and J T Baker, respectively. Titanium dioxide P-25 (mainly anatase ca. 50 $m^2 g^{-1}$ nonporous) was a gift from Degussa (Frankfurt, Germany). High purity water was obtained from a Maxima water purification system (USF-Elga, High Wycombo, Bucko, UK). Other chemicals are of analytical reagent grade.

2.2. Synthesis of 1-phenyl-3-hydroxy-1,2,4-triazole

The synthesis was carried out as reported previously [14] with some modification. Concentrated hydrochloric acid (0.121 g) was carefully added to a solution of 1-phenyl semicarbazide (0.121 g) in 85% formic acid (0.448 g) and water (0.213 mL). The mixture was heated for 4 h at 95 °C, after which time the mixture was diluted with water (10 mL), and the resulting precipitate filtered off under suction. The filter cake was washed neutral with water and dried with stream of air. Crude 1-phenyl-3-hydroxy-1,2,4-triazole was purified by column chromatography using dichloromethane as an eluent to yield pure 1-phenyl-3-hydroxy-1,2,4-triazole (0.025 g) having a melting point of 284–286 °C. ^{1}H NMR (400 MHz, MeOH-d_4, ppm): δ_H 8.77 (s, H-5), 7.71 (br d, J = 8.4 Hz, H-2′, H-6′), 7.50 (br t, J = 8.1 Hz, H-3′, H-5′), 7.37 (br t, J = 7.4 Hz, H-4′). ^{13}C-NMR (100 MHz, MeOH-d_4, ppm): δ_C 167.5 (C-3), 140.8 (C-5), 138.4 (C-1′), 130.9 (C-3′, C-5′), 129.1 (C-4′), 119.9 (C-2′, C-6′). ^{1}H and ^{13}C NMR spectra were obtained with a Bruker AVANCE 400 MHz spectrometer with solvent signal as internal reference.

2.3. Photocatalytic degradation studies

Irradiation was performed in Pyrex cylindrical cells using a Suntest apparatus from Heraeus (Hanau, Germany) equipped with a Xenon lamp with a flux of 550 W/m^2 and a special filter that eliminates the light with wavelength shorter than 290 nm. The 500 mL of triazophos (20 mg L^{-1}) solution containing 10 mg L^{-1} of TiO_2 was magnetically stirred before illumination for at least half an hour in the dark in order to achieve the maximum adsorption of the triazophos onto semiconductor surface. During experiment, the solution was magnetically stirred and sparged with air at the rate of 5.7 L min^{-1} and each 5 mL portion of samples was collected at specific time intervals. The degradation products were analyzed by HPLC-UV, IC, LC/MS/MS and GC/MS/MS. During the photocatalytic degradation of triazophos, the pH decreased from 6.9 to 4.9 because of the formation of acidic products.

2.4. Sample extraction for GC/MS/MS analysis

Aliquots of 5.0 mL were taken at each specific interval and filtered using a cellulose acetate membrane (0.20 μm) to remove TiO_2. The filtrate was extracted in dichloromethane (5 mL) and the extract was then evaporated under a gentle stream of nitrogen to dryness. The residue was redissolved in 200 μL in dichloromethane prior to injection to GC/MS/MS.

2.5. Separation of O,O-diethyl-O-1-phenyl-1H-1, 2,4-triazol-3-yl phosphoric acid (oxon derivative of triazophos)

To isolate the oxon derivative of triazophos (compound **2**) the photodegradation experiment was carried out as described above except that 25 mg/L triazophos was irradiated for 20 h. The irradiated aqueous solution was extracted with dichloromethane (500 mL). The extract was then evaporated to 2 mL, filtered using a nylon membrane (0.2 μm) and injected on a semipreparative column (PRP1, 7 mm × 305 mm, 10 μm, Hamilton) with a gradient elution of acetonitrile and water. The gradient started at 60% acetonitrile and increased linearly to 100% in 10 min, and held for further 10 min. The flow rate was set at 1 mL min^{-1}, the eluate was monitored at 250 nm, and the injection volume was 20 μL. Triazophos oxon fraction was collected at a retention time of 12.1 min. This experiment was repeated eight times. The combined eluate was extracted with dichloromethane. The extract was then evaporated to dryness. The product obtained was identified by NMR and mass spectroscopy. ^{1}H NMR (400 MHz, $CDCl_3$, ppm): δ_H 8.30 (s, H-5), 7.60 (d, J = 8.2 Hz, H-2′, H-6′), 7.48 (t, J = 7.9 Hz, H-3′, H-5′), 7.38 (t, J = 7.9 Hz, H-4′), 4.37 (q, J = 7.1 Hz, H-1″), 1.41 (t, J = 7.1 Hz, H-2″); ^{13}C-NMR (100 MHz, $CDCl_3$, ppm): δ_C 162.0 (C-3), 140.0 (C-5), 136.6 (C-1′), 129.3 (C-3′, C-5′), 127.5 (C-4′), 119.5 (C-2′, C-6′), 65.5 (C-1″), 16.0 (C-2″). Mass spectral data: m/z at 298$[M+H]^+$ (100), 270 (32), 242 (5), 162 (14).

2.6. Analytical measurements

2.6.1. HPLC–UV

HPLC analyses were carried out using a Perkin Elmer equipped with a Perkin Elmer series 200 IC pump, an Advanced LC Sample Processor ISS 200 and a Diode array 235 C (Wellesley, MA, USA). Data were processed using Navigator Version 4.0. A LiChrospher® 100 RP 18 column (4.6 mm × 250 mm, 5 μm, Merck) was used in a gradient elution of acetonitrile and water. The gradient started at 50% acetonitrile, linearly increased to 90% acetonitrile in 10 min at a flow rate of 1 mL min^{-1}. The eluate was monitored at 250 nm. The injection volume was 20 μL.

2.6.2. LC/MS/MS

The mass spectrometric detection was carried out using an Applied Biosystem API 2000 Triple quadrupole instrument

Table 1
Optimized parameter for MS/MS transition of triazophos and degradation products in the PI and NI modes[a]

Compound	MS/MS transition	DP (V)	FP (V)	EP (V)	CEP (V)	CE (V)	CXP (V)
Positive ionization mode							
Triazophos, *O*,*O*-diethyl-*O*-1-phenyl-1H-1,2,4-triazol-3-yl phosphorothioic acid (**1**)	314/162	25	350	−10	30	20	20
	314/119	25	350	−10	30	40	20
Triazophos oxon, *O*,*O*-diethyl-*O*-1-phenyl-1H-1,2,4-triazol-3-yl phophoric acid (**2**)	298/270	25	350	−10	30	20	15
	298/242	25	350	−10	30	20	14
	298/162	25	350	−10	30	30	7
O-Ethyl-*O*-1-phenyl-1H-1,2,4-triazol-3-yl phosphorothioic acid (**3**)	286/162	25	350	−10	30	40	15
	286/178	25	350	−10	30	30	15
	286/240	25	350	−10	30	20	15
1-Phenyl-3-hydroxy-1,2,4-triazole (**4**)	162/119	45	350	−10	28	25	16
	162/92	20	350	−10	28	30	10
O-Ethyl-*O*-1-phenyl-1H-1,2,4-triazol-3-yl phosphoric acid (**6**)	270/162	25	350	−10	30	25	7
	270/242	25	350	−10	30	20	7
N-Phenyl formamide (**7**)	121/121	40	350	−10	28	5	10
	121/93	40	350	−10	28	22	15
	93/66	40	350	−10	28	20	10
Carbonic acid amide (**8**)	61/61	40	350	−10	26	5	10
	61/44	40	350	−10	26	30	10
Aniline (**9**)	94/94	45	350	−10	27	5	7
	94/77	40	350	−10	27	20	10
Unknown	121/103	40	350	−10	27	28	15
	121/93	40	350	−10	27	22	15
Negative ionization mode							
O,*O*-Diethyl phosphorothioic acid (**5**)	169/169	−15	−350	10	−31	−5	−6
	169/141	−15	−350	10	−31	−20	−6
	169/95	−25	−350	10	−31	−20	−6
O-Ethyl phosphorothioic acid (**10**)	141/95	−15	−350	10	−32	−25	−6
	141/141	−20	−350	10	−32	−5	−6
O,*O*-Diethyl phosphoric acid (**11**)	153/79	−25	−350	10	−32	−20	−6
	153/125	−15	−350	10	−32	−22	−6
O-Ethyl phosphoric acid (**12**)	125/79	−20	−350	10	−33	−25	−6
	125/125	−20	−350	10	−33	−5	−6
Phosphoric acid (**13**)	97/97	−15	−350	10	−32	−22	−6
	97/79	−15	−350	10	−32	−15	−6

[a]Source parameter: curtain gas 45 psi, collision activated dissociation gas 3, ion spray voltage 1100 V (PI mode), −1100 V (NI mode), nebulizer gas 50 psi, heater gas 60 psi, temperature 350 °C.

(Thornhill, Toronto, Canada) equipped with a TurboIonSpray source. The Analyst software (1.1 version) was used for the system control and data acquisition. The optimized parameters for MS/MS are summarized in Table 1. The chromatographic separation was performed on a Synergi MAX-RP C12 column (Phenomenex, 4.6 mm × 150 mm i.d., 4 μm particle size). The mobile phase was methanol: 0.01% formic acid in 5 mM ammonium formate and the gradient elution for positive ionization mode started from 20% methanol and then increased linearly to 100% in 10 min then held for 5 min. The column was equilibrated under the initial condition for 5 min prior to the next

Table 2
Retention times (t_R) and parameters used in GC/MS/MS

Compound	MS/MS transition	t_R (min)	CE (V)
Aniline (**9**)	93/66	8.83	−10
N-Phenyl formamide (**7**)	121/66	14.02	−20
1-Phenyl-3-hydroxy-1,2,4-triazole (**4**)	161/133	18.65	−10
Triazophos oxon (**2**)	297/188	25.96	−30
Triazophos (**1**)	313/161	26.26	−20

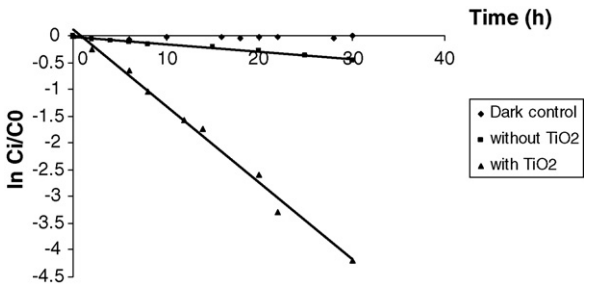

Fig. 2. The disappearance of triazophos under different conditions.

injection, at a flow rate of 0.3 mL min^{-1}. The gradient elution for negative ionization mode started from 30% methanol and then increased linearly to 50% in 5 min, to 100% in 1 min and then held for 9 min. The column was equilibrated under the initial condition for 7 min prior to the next injection, at a flow rate of 0.3 mL min^{-1}. Injection volume was 20 μL.

2.6.3. GC/MS/MS

A Varian 1200L Quadrupole GC/MS/MS (Walnut, Creek, USA) was employed. It consists of a Varian CP-3800 gas chromatograph with CP 8410 auto injector and coupled with a 1200L Quadrupole MS/MS detector. A Varian MS workstation version 6 was used for the system control and data acquisition. The optimized parameters for MS/MS are summarized in Table 2. Separations were performed on a capillary column (VF-5ms, 5% phenyl 95% dimethylpolysiloxane, 60 m × 0.32 mm i.d., 0.25 μm film thickness). The carrier gas was 99.999% helium at a flow rate of 1.0 mL min^{-1}. The injector temperature was set at 200 °C and 1.0 μL sample was injected in the split mode with

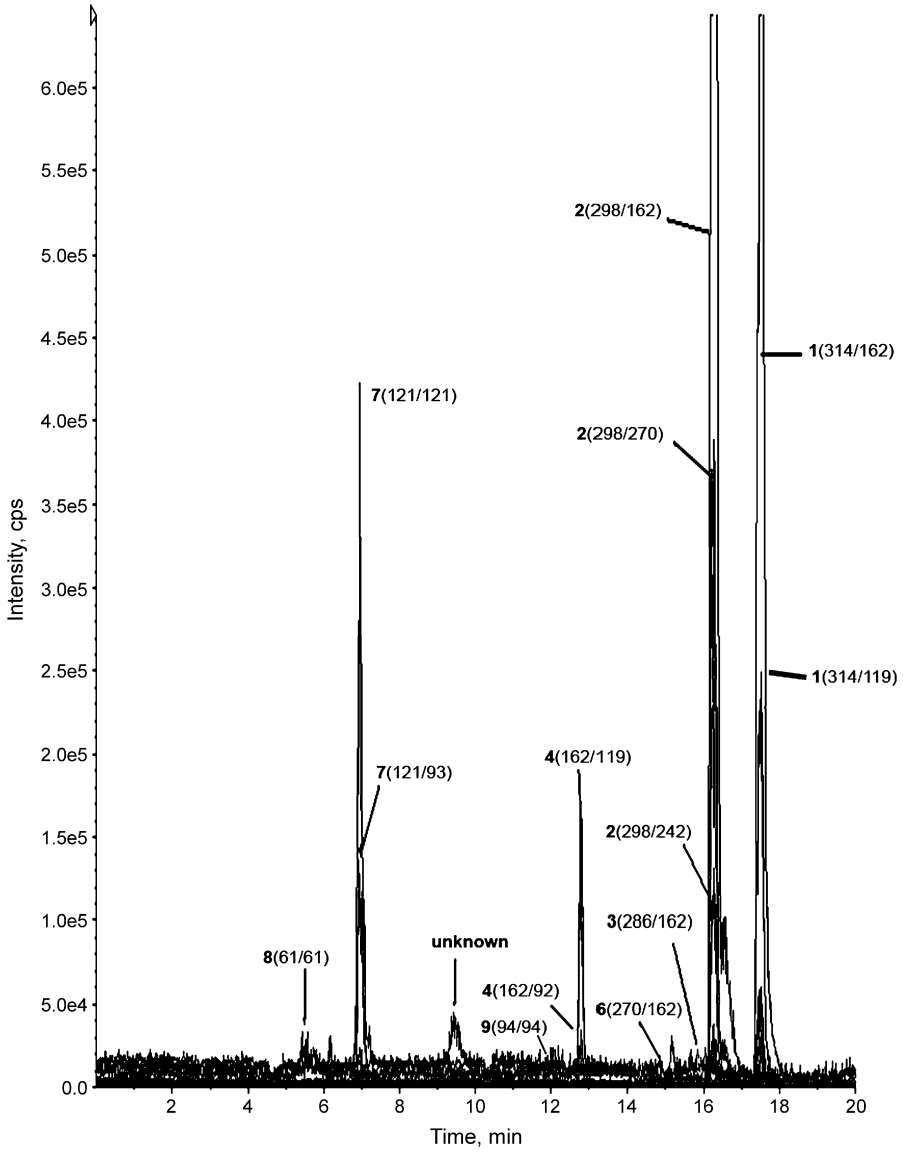

1 = triazophos, **2** = triazophos oxon, **3** = *O*-ethyl-*O*-1-phenyl-1H-1,2,4-triazol-3-yl phosphorothioic acid, **4** =1-phenyl-3-hydroxy-1,2,4-triazole, **6** = *O*-ethyl-*O*-1-phenyl-1H-1,2,4-triazol-3-yl phosphoric acid, **7** =N-phenyl formamide, **8** = carbonic acid amide, and **9** = aniline.

Fig. 3. Typical total ion chromatogram (MRM) of triazophos and its degradation products after 8 h of irradiation in positive ionization mode (LC/MS/MS). Numbers in parentheses are MRM transitions refer to Table 1.

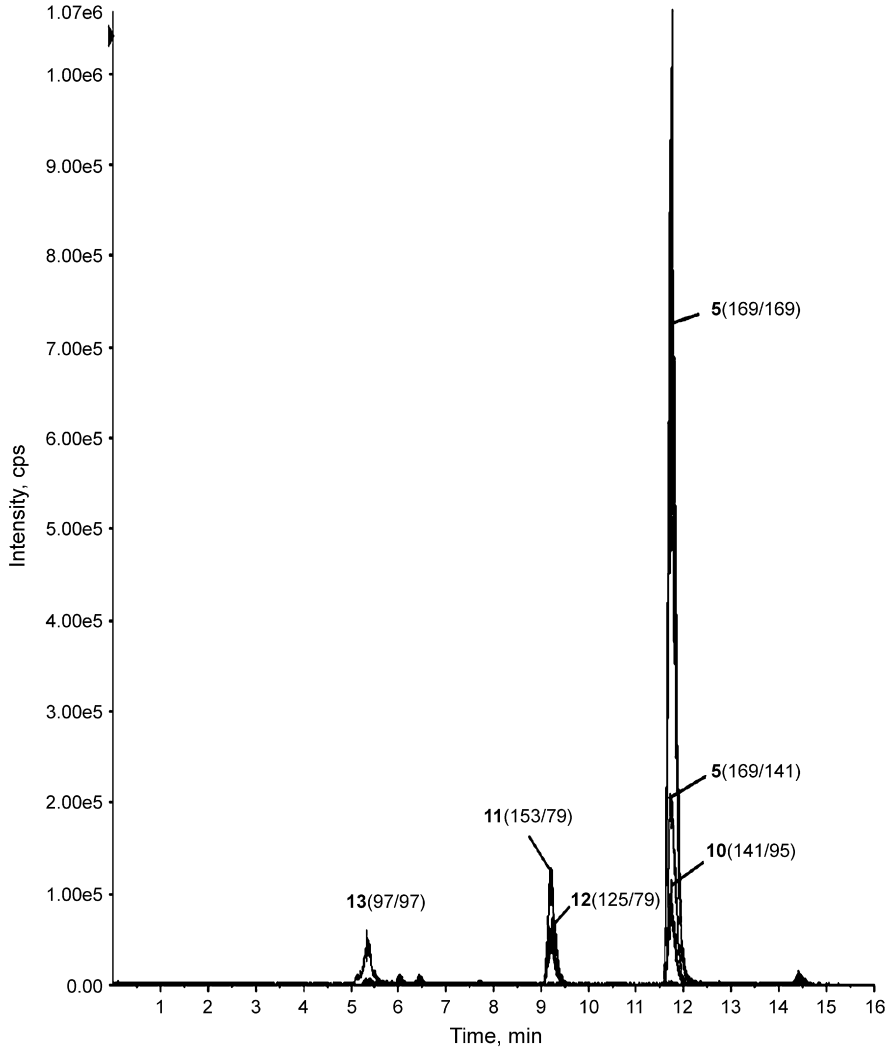

Fig. 4. Typical total ion chromatogram (MRM) of degradation products of triazophos 8 h of irradiation in negative ionization mode (LC/MS/MS). Numbers in parentheses are MRM transitions refer to Table 1.

a split ratio of 5:1. Samples were analyzed using the following temperature program with solvent delay time of 7 min, initial temperature of 50 °C increased by 10 °C min^{-1} to 250 °C, and to 270 °C by 2 °C min^{-1}. The source and transfer line temperatures were 200 and 250 °C, respectively. The emission current of the ionization filament was set to 50 μA generating electrons with 70 eV.

2.6.4. Ion chromatography

A Dionex 500 ion chromatograph, equipped with an Ion Pac® AS11-HC (2 mm × 250 mm) column, an automated potassium hydroxide eluent generator (EG40) and suppressed conductivity detector was employed to analyze inorganic degradation products. The potassium hydroxide gradients from 12 to 20 mM in 13 min and increase to 40 mM in 0.1 min then held for 20 min. The column was equilibrated under the initial condition for 15 min prior to the next injection. The flow rate and injection volume were 0.10 mL min^{-1} and 10 μL, respectively.

3. Results and discussion

3.1. Kinetic studies

To compare the rate of photolysis and photocatalytic degradation of triazophos, three sets of experiments were performed (Fig. 2). The dark control experiment was performed with triazophos and titanium dioxide in the absence of light, the second set by exposing triazophos to light, and the third set with triazophos and titanium dioxide in the presence of light.

The dark control experiment showed that no triazophos concentration change after 30 h while the exposure of triazophos in the absence of TiO_2 showed slow degradation with initial rate of 0.0137 h^{-1}. In the presence of light and TiO_2, the loss of triazophos was approximately ten times faster than that observed in the absence of TiO_2. The difference in the rate may be due to the production of oxidants by the irradiated TiO_2 catalyst [11,15–16].

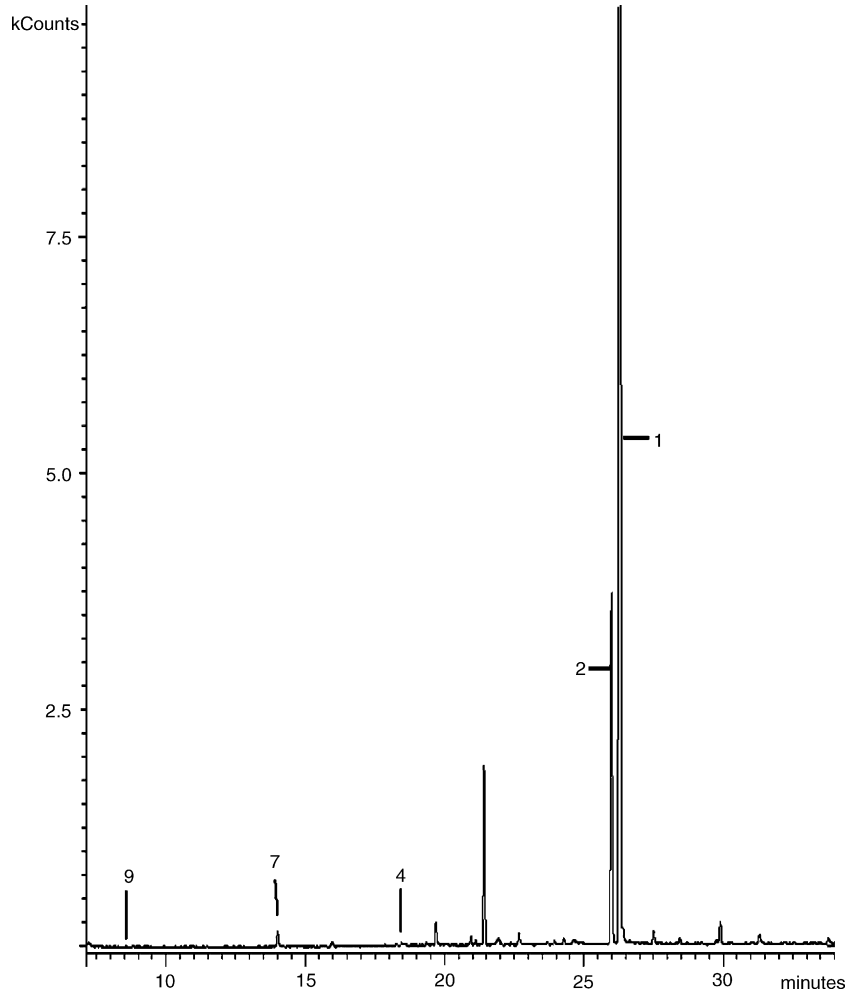

Fig. 5. Typical total ion chromatogram (MRM) of triazophos and its degradation products after 24 h of irradiation in EI mode (GC/MS/MS). Peak numbers: (**1**) triazophos, (**2**) triazophos oxon, (**4**) 1-phenyl-3-hydroxy-1,2,4-triazole, (**7**) *N*-phenyl formamide, and (**9**) aniline.

To assess the reproducibility of the method, experiments were repeated three times. The degradation rates were reproducible with r^2 values for plots of the natural log of triazophos concentration versus time exceeding 0.98 in every case. Under the conditions studied, the rate constant of photocatalytic degradation of triazophos at 20 ppm in the presence of 10 mg L^{-1} TiO_2 was $0.146 \pm 0.013\ h^{-1}$ and $T_{1/2}$ was 4.67 ± 0.42 h.

3.2. Intermediate studies

The products generated during the photocatalytic process were analyzed by LC/MS/MS, GC/MS/MS and IC. The intermediates were identified by comparison with commercially available authentic standards, by matching against a mass spectra library (GC/MS), and by interpretation of fragment ions obtained from Q1 and product ion scan, additionally in oxon case, identified by MS, ^1H and ^{13}C NMR spectroscopic data.

A full scan of TurboIonSpray-MS spectra obtained for all organic intermediate compounds showed $[M^+]$, $[M+H]^+$, and $[M-H]^-$ detected in positive and negative ionization modes, respectively. At the selected molecular ion or quasimolecular ion, the product ion scan was performed and collision activated dissociation gas (CAD) was switched on so that fragmentation of the chosen precursor ion could occur. Either one or two most abundant product ions were chosen followed by manual optimization of collision energy (CE) and collision cell exit potential (CXP) for each of the two MS/MS transitions. The

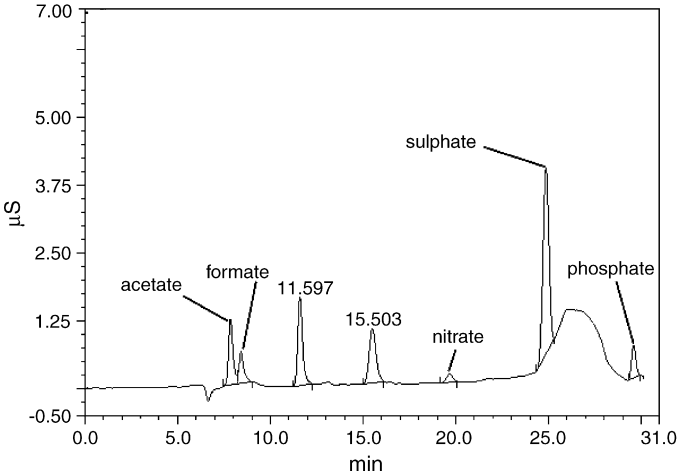

Fig. 6. Typical ion chromatogram of degradation products of triazophos 8 h irradiation.

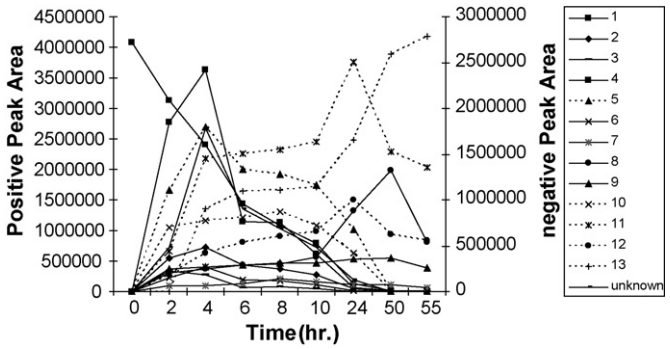

Fig. 7. Degradation of triazophos and the subsequent formation and disappearance of products as a function of irradiation time during TiO_2 photocatalysis. The solid lines refer to the left ordinate and profiles of triazophos and its degradation products detected in positive ionization mode. The dotted lines refer to the right ordinate and profiles of degradation products of triazophos detected in negative ionization mode.

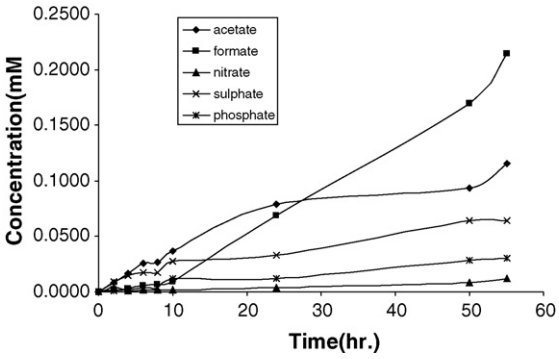

Fig. 8. Evolution of low molecular weight organic acid and mineral acid anions from triazophos after 8 h of irradiation.

time profile of triazophos and its degradation products were then monitored in multireaction monitoring (MRM) mode as it provides much higher sensitivity than both Q1 scan and product ion scan modes. Typical total ion chromatograms (MRM) of triazophos and degradation products in positive and negative ionization modes are as shown in Figs. 3 and 4, respectively. Aniline and N-phenyl formamide, 3-hydroxy-1-phenyl-1,2,4-triazole, triazophos oxon and triazophos were also detected by GC/MS/MS (Fig. 5). *N*-Phenyl formamide was also identified using the identification program of NIST library with *R* match of 844 and *F* match of 805. The match of not very high score may be due to the coelution of an unknown compound, which was evident by LC/MS/MS (Fig. 3). Formate, acetate, nitrate,

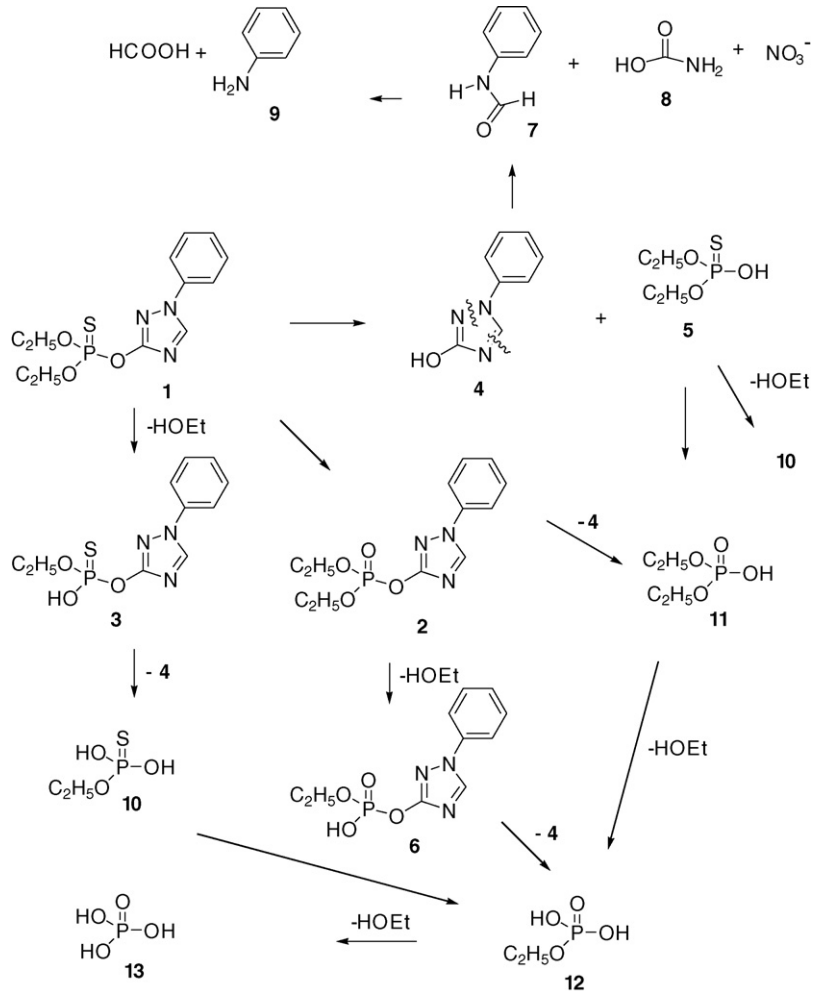

Scheme 1. Various detected degradation products of triazophos.

Table 3
Retention times (t_R) and MS characteristics of intermediates detected by LC/MS

Compound	t_R (min)	MS data (*m/z*)
Positive ionization mode		
Triazophos (**1**)	17.44	314 $[M+H]^+$, 286 $[M+H-C_2H_4]^+$,178 $[C_8H_8N_3S]^+$, 162 $[C_8H_8N_3O]^+$,119 $[162\text{-}CNOH]^+$
Triazophos oxon (**2**)	16.22	298 $[M+H]^+$, 270 $[M+H\text{-}C_2H_4]^+$,242 $[M+H\text{-}2\ C_2H_4]^+$, 162 $[C_8H_8N_3O]^+$
O-Ethyl-*O*-1-phenyl-1H-1,2,4-triazol-3-yl-phosphorothioic acid (**3**)	15.90	286 $[M+H]^+$, 258 $[M+H\text{-}C_2H_4]^+$, 240 $[M+H\text{-}C_2H_5OH]^+$, 178 $[C_8H_8N_3S]^+$, 162 $[C_8H_8N_3O]^+$
1-Phenyl-3-hydroxy-1,2,4-triazole (4)	12.75	162 $[M+H]^+$, 119 $[M+H\text{-}CNOH]^+$, 92 $[M\text{-}C_2H_2N_2O]^+$, 77 $[C_6H_5]^+$
O-Ethyl-*O*-1-phenyl-1H-1,2,4-triazol-3-yl phosphoric acid (**6**)	14.87	270 $[M+H]^+$, 242 $[M+H\text{-}C_2H_4]^+$,223 $[M-C_2H_5OH]^+$, 162 $[C_8H_8N_3O]^+$
N-Phenyl formamide (**7**)	6.93	121 $[M]^+$, 93$[M-CO]$, 66 $[C_5H_6]^+$
Carbonic acid amide (**8**)	5.43	61 $[M+H]^+$, 44 $[M+H\text{-}NH_3]^+$
Aniline (**9**)	11.98	94 $[M+H]^+$, 77 $[C_6H_5]^+$
Unknown	9.43	121, 103, 93, 66
Negative ionization mode		
O,*O*-Diethyl phosphorothioic acid (**5**)	11.56	169 $[M-H]^-$, 141 $[M-H\text{-}C_2H_4]^-$,113$[M-H\text{-}2C_2H_4]^-$, 95$[M-H\text{-}C_2H_4\text{-}C_2H_5OH]^-$
O-Ethyl phosphorothioic acid (**10**)	11.56	141 $[M-H]^-$, 113 $[M-H\text{-}C_2H_4]^-$,95 $[M-H\text{-}C_2H_5OH]^-$
O,*O*-Diethyl phosphoric acid (**11**)	9.20	153 $[M-H]^-$, 125 $[M-H\text{-}C_2H_4]^-$, 79 $[M-H\text{-}C_2H_4\text{-}C_2H_5OH]^-$
O-Ethyl phosphoric acid (**12**)	9.20	125 $[M-H]^-$, 79 $[M-H\text{-}C_2H_5OH]^-$
Phosphoric acid (**13**)	5.28	97 $[M-H]^-$, 79 $[M-H_2O]^-$

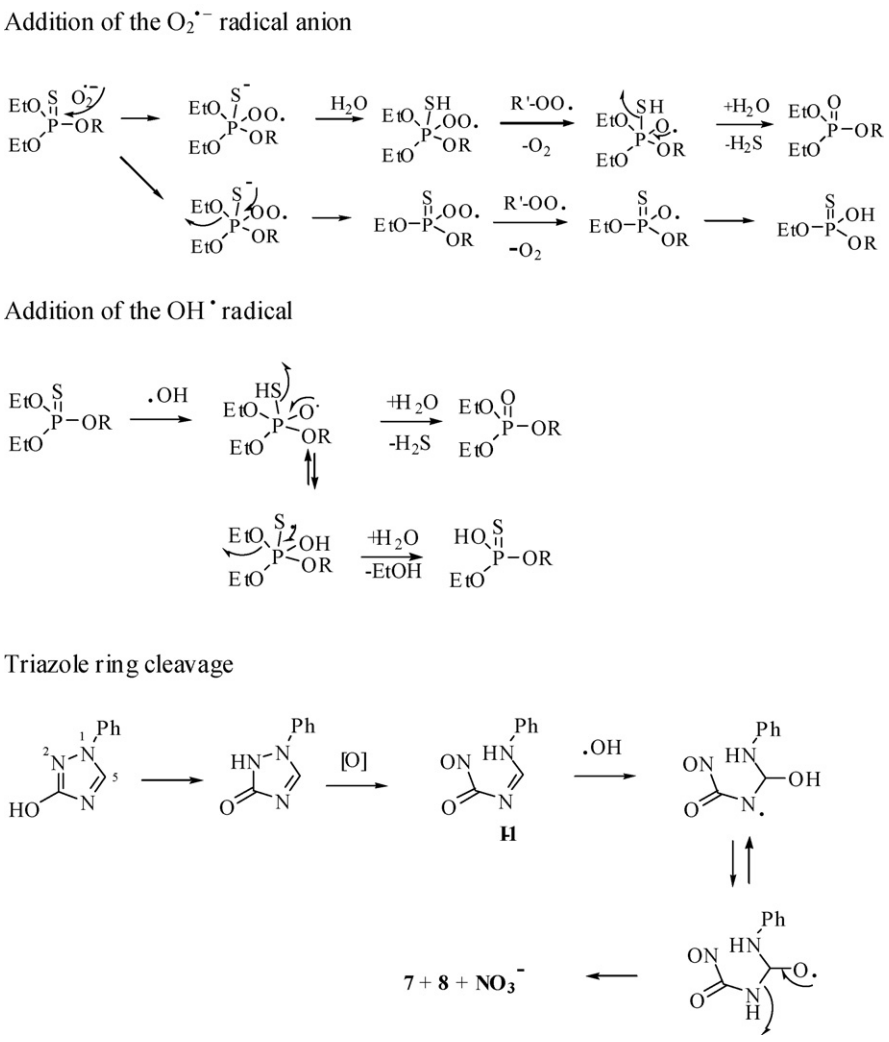

Scheme 2. Proposed photocatalytic transformations of triazophos in aqueous solution.

sulphate and phosphate were detected by ion chromatography (Fig. 6). The remarkable increase of the baseline during retention time 25–30 min could be due to the carbonate ion formed from carbon dioxide present in the sample and hydroxide mobile phase and due to the gradient elution. The details of spectral data are shown in Table 3.

At least two MRM transitions were used to monitor the degradation of triazophos and its products whenever it is possible. This made the time profile obtained accurate since detection by MRM mode is very selective. The time profile for the disappearance of triazophos and the formation of the organic products and phosphate during photocatalysis is illustrated in Fig. 7.

Compounds were regarded as intermediate products provided that their concentrations initially increased and subsequently decreased after prolonged irradiation. The formation of the triazophos oxon (compound **2**) suggests that it is an intermediate in the degradation that in turn was further transformed into new photoproducts as described in Schemes 1 and 2. This is consistent with the hypotheses that sulfate is produced by an oxidative attack of the hydroxyl radical or a similar oxidizing species on the P=S bond [17]. As shown in Fig. 7, phosphate (compound **13**) evolution coincides with triazophos (compound **1**) degradation.

A complete degradation of an organic molecule by photocatalysts normally leads to the conversion of all its carbon atoms to gaseous carbon dioxide [7], and the hetero atoms into inorganic anions, that is nitrate, sulphate and phosphate that remain in solutions as shown in Fig. 8.

In the later stage of the reaction, acetic acid was likely produced by oxidation of ethanol formed after ester bond cleavage. At 24 h irradiation time, a mass balance between the triazophos consumed and sulphate evolved was found to be 53% and increased to 100% at 50 h of total irradiation time. This confirms the hypotheses that the transformation products could occur via two routes (see Schemes 1 and 2). The ca. 100% sulphate mass balance occurs at much longer illumination time than the disappearance of triazophos.

3.3. Proposed photocatalytic degradation pathways

Various degradation products of triazophos were detected as shown in Scheme 1.

Formation of oxon (**2**) from triazophos (**1**), and hydrolytic cleavage of any of the P–O bonds in either **1** or **2** that can lead to several intermediates were proposed to arise by attack of the $O_2^{\bullet -}$ radical anion at the phosphorus atom of **1** as shown in Scheme 2. Hydrogen sulphide, although not detectable, was proposed as one of possible intermediates that can be further transformed to sulphate. Another addition–elimination mechanism in which the hydroxyl radical adds to the phosphorus atom, followed by the elimination of ethoxy or alkoxy group can also be one of the probable pathway [18]. Cleavage of the triazole ring, as evident from the detections of **7** and **9**, was proposed from oxidation at the N atom bearing higher partial negative charge, N-2, which led to N-1-N-2 bond scission and resulting in the formation of intermediate I-**1** [19]. Attack of the hydroxy radical at C-5 in I-**1** with subsequent rearrangement, could cause C-5-N-4 bond cleavage leading to formic acid amide (**7**), carbonic acid amide (**8**) and nitrate. Further transformation of amides gave the corresponding acids, ammonia and aniline (**9**). None of phenyl semicarbazide, phenyl hydrazine, phenol and urea was detected in this study.

4. Conclusions

The photocatalytic degradation of triazophos in aqueous TiO_2 suspension has been studied by using simulated sunlight. The degradation rate of triazophos followed first-order kinetics at a rate that was much faster than that of direct photolysis. Seventeen degradation products were identified and transformation routes of the photocatalytic degradation of triazophos were proposed. Photocatalytic degradation of triazophos shows great promise as a cost-effective treatment technology. Additional research is needed to assess the effect of natural water constituents (e.g., humic substances) on the rate of triazophos degradation as well as the economics of the treatment system.

Acknowledgements

Financial support from Postgraduate Education and Research Program in Chemistry (PERCH), the German Academic Exchange Service (DAAD)-Thailand Research Fund through the Royal Golden Jubilee Ph.D. Program, Alexander von Humboldt Stiftung and Kasetsart University Research and Development Institute are gratefully acknowledged. The authors thank Professor David L. Sedlak for the helpful discussion.

References

[1] C.R. Worthing, R.J. Hanrce, The pesticide manual: a world compendium, ninth ed., British Crop Protection Council, Surrey, 1991, p. 838.
[2] Q. Mingjing, H. Zhaojun, X. Xinjun, Y. Lina, Triazophos resistance mechanisms in the rice stem borer (*Chilo suppressalis* Walker), Pesticide Biochem. Physiol. 77 (2003) 99–105.
[3] S. Rani, V.K. Madan, T.S. Kathpal, Persistence and dissipation behavior of triazophos in canal water under Indian climatic conditions, Ecotoxicol. Environ. Saf. 50 (2001) 82–84.
[4] K. Lin, D. Yuan, M. Chen, Y. Deng, Kinetics and products of photo-Fenton degradation of triazophos, J. Agric. Food Chem. 52 (2004) 7614–7620.
[5] K. Lin, D. Yuan, M. Chen, Y. Deng, Hydrolytic products and kinetics of triazophos in buffered and alkaline solutions with different values of pH, J. Agric. Food Chem. 52 (2004) 5404–5411.
[6] S. Devipriya, S. Yesodharan, Photocatalytic degradation of pesticide contaminants in water, Sol. Energy Mat. Sol. Cell 86 (2005) 309–348.
[7] L. Muszkat, Photochemical processes, in: P. Kearney, T. Roberts (Eds.), Pesticide Remediation in Soils and Water, Wiley, New York, 1998, pp. 307–337.
[8] M. Mahalakshmi, B. Arabindoo, M. Palanichamy, V. Murugesan, Photocatalytic degradation of carbofuran using semiconductor oxides, J. Hazard. Mater. 143 (2007) 240–245.
[9] X. Zhu, X. Feng, C. Yuan, X. Cao, J. Li, Photocatalytic degradation of pesticide pyridaben in suspension of TiO_2: identification of intermediates and degradation pathways, J. Mol. Catal. A Chem. 214 (2004) 293–300.
[10] P. Calza, C. Medana, C. Baiocchi, E. Pelizzetti, Photocatalytic transformations of aminopyrimidines on TiO_2 in aqueous solution, Appl. Catal. B Environ. 52 (2004) 267–274.
[11] T.M. Sakellarides, M.G. Siskos, T.A. Albanis, Photodegradation of selected organophosphorus insecticides under sunlight in different natural waters and soils, Int. J. Environ. Anal. Chem. 83 (2003) 33–50.

[12] H.D. Burrows, M.L. Canle, J.A. Santaballa, S. Steenken, Reaction pathways and mechanisms of photodegradation of pesticides, J. Photochem. Photobiol. B Biol. 67 (2002) 71–108.

[13] J.M. Hermann, C. Guillard, M. Arguello, A. Agüera, A. Tejedor, L. Piedra, A. Fernández-Alba, Photocatalytic degradation of pesticide pirimiphos-methyl, determination of the reaction pathway and identification of intermediate products by various analytical methods, Catal. Today 54 (1999) 353–367.

[14] M. Koch, G. Staehler, Process for the manufacture of substituted 3-hydroxy-1,2,4-triazoles U.S. Patent 4,467,098 (1984).

[15] E. Vulliet, C. Emmelin, M.F. Grenier-Loustallot, O. Païssé, J.M. Chovelon, Simulated sunlight-induced photodegradations of triasulfuron and cinosulfuron in aqueous solutions, J. Agric. Food Chem. 50 (2002) 1081–1088.

[16] G. Goutailler, C. Guillard, R. Faure, O. Païssé, Degradation pathway of dicyclanil in water in the presence of titanium dioxide. Comparison with photolysis, J. Agric. Food Chem. 50 (2002) 5115–5120.

[17] T.-S. Kim, J.-K. Kim, K. Choi, M.K. Stenstorm, K.-D. Zoh, Degradation mechanism and the toxicity assessment in TiO_2 photocatalysis and photolysis of parathion, Chemosphere 62 (2006) 926–933.

[18] K.E. O'Shea, S. Beightol, I. Garcia, M. Aquilar, D.V. Kalen, W.J. Cooper, Photocatalytic decomposition of organophosphonates in irradiated TiO_2 suspensions, J. Photochem. Photobiol. A Chem. 107 (1997) 221–226.

[19] N. Watanabe, S. Horikoshi, A. Kawasaki, H. Hidaka, Formation of refractory ring-expanded Triazine intermediate during the photocatalyzed mineralization of the endocrine disruptor amitrole and related triazole derivatives at UV-irradiated TiO_2/H_2O interfaces, Environ. Sci. Technol. 39 (2005) 2320–2326.